Modeling the Risk of a Failed Wind Turbine Blade Impacting a Power Transmission Line

Nathan Slegers[1], Jonathan Rogers[2], Mark Costello[*,3], Maria Puga[4] and Patricia Arons[5]
[1]Mechanical and Aerospace Engineering, University of Alabama in Huntsville, Huntsville, AL 35899, USA
[2]School of Aerospace Engineering, Georgia Institute of Technology, Atlanta, GA 30332, USA
[3]School of Aerospace Engineering, Georgia Institute of Technology, Atlanta, GA 30332, USA
[4]Transmission and Interconnection Planning, Southern California Edison Company, Rosemead, CA 91770, USA
[5]Transmission and Interconnection Planning, Southern California Edison Company, Rosemead, CA 91770, USA

ABSTRACT

Wind turbine installations are generally situated in proximity to power transmission lines that integrate generated power into the grid. Failure of a wind turbine that results in a blade or blade fragment thrown from the rotor can result in impact with a transmission line and lead to significant transmission line damage. The work reported here creates a mathematical model to assess the risk of this type of failure event occurring as a function of wind turbine characteristics and the relative position of the power transmission line. A comprehensive rotor blade flight dynamic simulation tool comprised of a rigid body representation with 6 degrees of freedom is used. The model generates full three dimensional motion of a failed wind turbine blade from release of the wind turbine blade at the point of failure to impact. Monte Carlo simulation is used to generate impact statistics including the probability that a failed wind turbine blade will impact a transmission line. A set of simulation results are generated for a nominal 1.5 MW wind turbine with a 50 m transmission height. Simulation results show that large blade fragments have relatively high transmission line impact probabilities for small offset distances while small blade fragments have overall lower impact probabilities but are spread over a larger offset distance range. Transmission line impact probability is also a strong function not only of the offset distance but also the orientation of the transmission line relative to the wind turbine and the atmospheric wind velocity vector.

1. INTRODUCTION

The focus on generating more power from green renewable energy sources has motivated a push toward increasing the use of wind energy systems and integrating this power source into electric utility grids. Quite often, some wind turbines in a given wind farm are located near power transmission lines. Additionally, there is increasing pressure to pack more turbines into a given wind farm to increase power output from a particular parcel of land, leading to more turbines nestled close to power transmission lines. One concern when wind farms and power

*Corresponding to: Mark Costello, Sikorsky Associate Professor, School of Aerospace Engineering, Georgia Institute of Technology, Atlanta, GA 30332, USA.
E-mail: mark.costello@ae.gatech.edu

transmission lines are in close proximity is failure of a rotor blade resulting in a blade throw and its potential impact with a power transmission line. For wind turbine site determination, the risk of a failed wind turbine impacting a transmission line needs to be considered to assess whether a particular wind turbine and transmission line configuration provides an appropriate risk level to all parties involved.

Reliability analysis of large wind turbine systems as a whole has been recently reported by Tavner, Xiang, and Spinato [1]. Perhaps the first analysis of the wind turbine blade throw problem was undertaken by Eggwertz, Carlsson, et al [2] where the blade was released at various azimuthal locations and separated at various blade radial positions. Fragments were dynamically modeled as point masses with aerodynamic drag. Results indicate that ground impact past 1.8 times the overall turbine height was low. A similar dynamic model was developed and exercised by Macqueen and Ainsilie [3] where it was shown that the probability of a person being struck by a rotor fragment at a distance of 220 m was about the same as the probability of being struck by lightning. Turner [4] also employed a point mass flight dynamic model for a blade fragment, but used Monte Carlo simulation to construct a statistical distribution of blade fragment impact points. More recently, Eggers, Holley, et al [5] used a point mass dynamic model connected to Monte Carlo simulation and achieved results similar to Macqueen and Ainsilie [3]. Montgomerie [6] expanded the work of others [2–5] by dynamically modeling fragments with a rigid 6 degree of freedom dynamic model representation. Very large throw distances are shown which fall out of the range of most other reported efforts. A similar dynamic modeling approach is reported by Sorensen [7, 8] where parametric sensitivities on the maximum range of a fragment is given as a function of airfoil data, center of gravity location, blade pitch angle, and wind velocity. Turner [9] followed initial work with a point mass dynamic model with a rigid representation and obtained results like Sorensen [8, 9].

This article examines the probability that a failed wind turbine blade released into the atmosphere will impact a power transmission line. This is accomplished by using a comprehensive flight dynamic model comprised of a rigid body representation with 6 degrees of freedom. The model generates full three dimensional motion of a failed wind turbine blade from release of the wind turbine blade at the point of failure to impact. At the instant that the rotor blade breaks, the blade has a specific position, orientation, velocity, and angular velocity which are used as initial conditions for the flight dynamic simulation. Motion of the failed wind turbine blades are driven by the initial conditions at failure, gravity, and aerodynamic forces and moments. By coupling the flight dynamic model with statistical Monte Carlo simulation techniques, statistics on the probability of a blade fragment impacting a power transmission line are generated. Parametric trade studies are reported to examine transmission line impact probability as a function of wind turbine size, transmission line height, location, and orientation.

2. DYNAMIC MODEL OF A ROTOR BLADE FAILURE

2.1. Blade Equations of Motion

The flight dynamic simulation predicts position, orientation, velocity, and angular velocity of a failed wind turbine rotor blade from the instant in time when the blade breaks free from the tower until impact. During this time period the rotor blade is in atmospheric free flight. At the instant that the rotor blade breaks, the blade has a specific position, orientation, velocity, and angular velocity which are used as initial conditions for the flight dynamic simulation.

The numerical simulation employed in this study consists of a rigid body six degree of freedom model typically utilized in flight dynamic modeling of air vehicles and projectiles. The degrees of freedom include three position components of the mass center as well as four quaternion orientation parameters of the body. Quaternions are employed in place of Euler

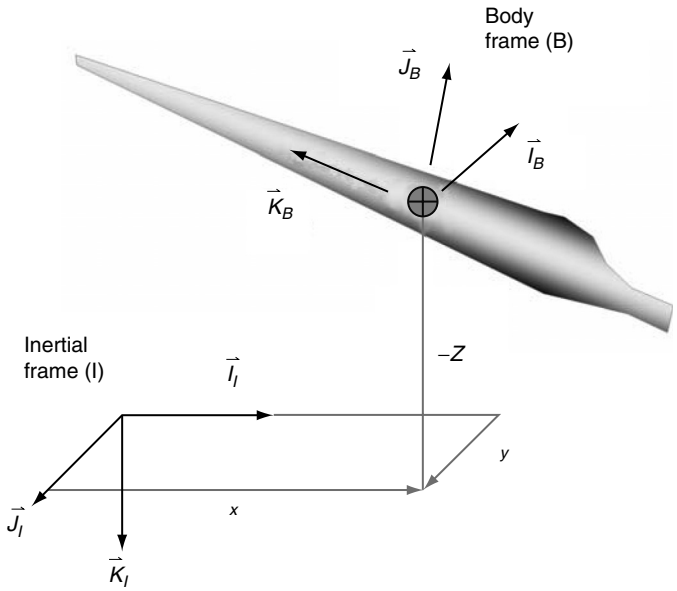

Figure 1: Flight dynamic model coordinates.

angles to avoid singularity problems in the kinematic differential equations since the body can take on an arbitrary orientation during flight. The ground is used as an inertial frame and the body frame is located at the rotor blade mass center with the $\vec{K}_B$ axis aligned with the axis of symmetry while the $\vec{I}_B$ and $\vec{J}_B$ axes form a right-handed coordinate system. A schematic of the body in flight is given in Figure 1 with the inertial and body reference frames labeled.

The resulting thirteen differential equations of motion describing the flight dynamics of the system, including the translation kinematics, rotation kinematics, translation dynamics, and rotation dynamics, are given by Equations 1 through 4. In these equations, (x, y, z) denote the mass center position, (q_0, q_1, q_2, q_3) are the quaternion orientation parameters, (u, v, w) are the body frame components of velocity, and (p, q, r) are the body frame components of angular velocity.

$$\begin{Bmatrix} \dot{x} \\ \dot{y} \\ \dot{z} \end{Bmatrix} = [T_{IB}] \begin{Bmatrix} u \\ v \\ w \end{Bmatrix} \tag{1}$$

$$\begin{Bmatrix} \dot{q}_0 \\ \dot{q}_1 \\ \dot{q}_2 \\ \dot{q}_3 \end{Bmatrix} = \frac{1}{2} \begin{bmatrix} 0 & -p & -q & -r \\ p & 0 & r & -q \\ q & -r & 0 & p \\ r & q & -p & 0 \end{bmatrix} \begin{Bmatrix} q_0 \\ q_1 \\ q_2 \\ q_3 \end{Bmatrix} \tag{2}$$

$$\begin{Bmatrix} \dot{u} \\ \dot{v} \\ \dot{w} \end{Bmatrix} = \begin{Bmatrix} X/m \\ Y/m \\ Z/m \end{Bmatrix} - \begin{bmatrix} 0 & -r & q \\ r & 0 & -p \\ -q & p & 0 \end{bmatrix} \begin{Bmatrix} u \\ v \\ w \end{Bmatrix} \tag{3}$$

$$\begin{Bmatrix} \dot{p} \\ \dot{q} \\ \dot{r} \end{Bmatrix} = [I]^{-1} \left(\begin{Bmatrix} L \\ M \\ N \end{Bmatrix} - \begin{bmatrix} 0 & -r & q \\ r & 0 & -p \\ -q & p & 0 \end{bmatrix} [I] \begin{Bmatrix} p \\ q \\ r \end{Bmatrix} \right) \tag{4}$$

Notice that *X, Y, Z* are the body frame components of the total applied forces while *L, M, N* represent the body frame applied moments about the mass center. The mass of the rotor blade is denoted as *m*. The matrix $[T_{IB}]$ is the body to inertial frame rotation transformation matrix given by

$$[T_{IB}] = \begin{bmatrix} q_0^2 + q_1^2 - q_2^2 - q_3^2 & 2q_1q_2 - 2q_0q_3 & 2q_1q_3 + 2q_0q_2 \\ 2q_1q_2 + 2q_0q_3 & q_0^2 - q_1^2 + q_2^2 - q_3^2 & 2q_2q_3 - 2q_0q_1 \\ 2q_1q_3 - 2q_0q_2 & 2q_2q_3 + 2q_0q_1 & q_0^2 - q_1^2 - q_2^2 + q_3^2 \end{bmatrix} \tag{5}$$

and $[I]$ is the mass moment of inertia matrix of the body evaluated at the mass center with respect to body frame coordinates.

$$[I] = \begin{bmatrix} I_{XX} & I_{XY} & I_{XZ} \\ I_{XY} & I_{YY} & I_{YZ} \\ I_{XZ} & I_{YZ} & I_{ZZ} \end{bmatrix} \tag{6}$$

The applied loads in equation 3 contain contributions from weight (W) and rotor blade aerodynamics (R).

$$\begin{Bmatrix} X \\ Y \\ Z \end{Bmatrix} = \begin{Bmatrix} X_W \\ Y_W \\ Z_W \end{Bmatrix} + \begin{Bmatrix} X_R \\ Y_R \\ Z_R \end{Bmatrix} \tag{7}$$

The weight contribution expressed in the body fixed frame is given by

$$\begin{Bmatrix} X_W \\ Y_W \\ Z_W \end{Bmatrix} = mg \begin{Bmatrix} 2q_1q_3 - 2q_0q_2 \\ 2q_2q_3 + 2q_0q_1 \\ q_0^2 - q_1^2 - q_2^2 + q_3^2 \end{Bmatrix} \tag{8}$$

The total aerodynamic force due to a rotor blade is calculated by discretizing the rotor blade into blade element segments and subsequently summing the aerodynamic forces on each blade element to form the total aerodynamic force and moment on the rotor blade

$$\begin{Bmatrix} X_R \\ Y_R \\ Z_R \end{Bmatrix} = \sum_{i=1}^{NR} \left(\begin{Bmatrix} X_{Ri} \\ Y_{Ri} \\ Z_{Ri} \end{Bmatrix} \right) \tag{10}$$

where

$$\begin{Bmatrix} X_{Ri} \\ Y_{Ri} \\ Z_{Ri} \end{Bmatrix} = \frac{1}{2} \rho \left(u_i^2 + v_i^2 \right) c_i dr_i \begin{Bmatrix} -C_{Li}\cos(\alpha_i - \delta_i) - C_{Di}\sin(\alpha_i - \delta_i) \\ C_{Li}\sin(\alpha_i - \delta_i) - C_{Di}\cos(\alpha_i - \delta_i) \\ 0 \end{Bmatrix} \tag{11}$$

In the above equation, ρ is the air density and δ_i is the i^{th} blade element pitch angle which includes blade twist. The i^{th} airfoil section lift and drag coefficients are denoted by C_{Li} and C_{Di} and are a function of section aerodynamic angle of attack α_i where

$$\alpha_i = \delta_i + \tan^{-1}\left(\frac{u_i}{v_i} \right) \tag{12}$$

Since the blade in free flight is likely to attain a general orientation as it tumbles to the ground, the aerodynamic angle of attack of the blade sections are likely to attain arbitrary

aerodynamic angles of attack. Thus, computationally the aerodynamic lift and drag coefficients are computed with a table look-up scheme with angle of attack entries from 180 deg to –180 deg. The velocity components utilized to compute the aerodynamic blade loads include motion of the blade section and atmospheric wind velocity and are written as

$$\begin{Bmatrix} u_i \\ v_i \\ w_i \end{Bmatrix} = \begin{Bmatrix} u + u_A - r_x r + r_z q \\ v + v_A + r_x r - r_z p \\ w + w_A - r_x q + r_y p \end{Bmatrix} \tag{13}$$

The blade element mass center offset distances are written as

$$\begin{Bmatrix} r_x \\ r_y \\ r_z \end{Bmatrix} = \begin{Bmatrix} SL_i \\ BL_i \\ WL_i \end{Bmatrix} - \begin{Bmatrix} SL_{CG} \\ BL_{CG} \\ WL_{CG} \end{Bmatrix} \tag{14}$$

using the notation *SL, BL, WL* denotes distance components along the $\vec{I}_B$, $\vec{J}_B$, and $\vec{K}_B$ axis, respectively. The relative aerodynamic velocity components (u_A, v_A, w_A) used in equations (13) are influenced by the atmospheric winds. The mean atmospheric wind acts in the horizontal ground plane with a magnitude of V_{MW} directed at an angle ψ_{MW} from the $\vec{I}_I$ axis and can be written as

$$\vec{V}_{MW} = V_{MW}\cos(\psi_W)\,\vec{i}_I + V_{MW}\sin(\psi_W)\,\vec{j}_I \tag{15}$$

Thus, the atmospheric wind velocity components in the rotor blade reference frame are given by

$$\begin{Bmatrix} u_A \\ v_A \\ w_A \end{Bmatrix} = \left[T_{IB}\right]^T \begin{Bmatrix} V_{MW}\cos(\psi_W) \\ V_{MW}\sin(\psi_W) \\ 0 \end{Bmatrix} \tag{16}$$

Since the aerodynamic force is not located at the mass center, it produces a moment about the mass center. Also, since the computation point of the rotor blade segment is not the aerodynamic center, an aerodynamic moment is also present. The aerodynamic moment due to the rotor blade contains contributions from both sources and is written as

$$\begin{Bmatrix} L_{R_i} \\ M_{R_i} \\ N_{R_i} \end{Bmatrix} = \frac{1}{2}\,\rho\left(u_i^2 + v_i^2\right)\,c_i^2 dr_i \begin{Bmatrix} 0 \\ 0 \\ C_{M_i} \end{Bmatrix} + \begin{Bmatrix} r_x Z_{R_i} - r_z Y_{R_i} \\ r_z X_{R_i} - r_x Z_{R_i} \\ r_x Y_{R_i} - r_y X_{R_i} \end{Bmatrix} \tag{17}$$

The total moment due to the rotor blade is the summation of these loads from all blade elements.

$$\begin{Bmatrix} L_R \\ M_R \\ N_R \end{Bmatrix} = \sum_{i=1}^{NR} \left(\begin{Bmatrix} L_{Ri} \\ M_{Ri} \\ N_{Ri} \end{Bmatrix} \right) \tag{18}$$

Given initial conditions for the rotor blade at the instant of failure the flight dynamic model described above is numerically integrated forward in time until the rotor blade impacts the ground. The flight dynamic simulation model is essentially the kernel that drives the overall analysis process. The simulation software has been optimized to run rapidly, allowing thousands of different failure events to be simulated in an automated fashion.

2.2. System Geometry

The overhead view of the transmission line and wind turbine system geometry is shown in Figure 2. The vertical axis of rotation of the wind turbine unit locates the horizontal position of the inertial frame origin. The vertical origin of the inertial reference frame is the ground. The wind turbine housing is rotated about the $\vec{K}_I$, axis by the angle ψ_T to arrive at the intermediate reference frame 1. The atmospheric wind acts in the horizontal ground plane and is rotated off the $\vec{I}_1$ axis by the angle ψ_W. The transmission line is modeled as a line in space that is parallel to the ground surface. The transmission line is rotated about the $\vec{K}_C$ axis by the angle ψ_C. The point C (x_c, y_c, z_c) is a point on the transmission line.

The center of rotation of the wind turbine rotor is located at point H. Its position vector from the origin of the inertial reference frame is given as

$$\vec{r}_{O\to H} = x_H\vec{I}_I + y_H\vec{J}_I + z_H\vec{K}_I = l\cos(\psi_T)\vec{I}_I + l\sin(\psi_T)\vec{J}_I - h\vec{K}_I \tag{19}$$

The rotor disk can be canted about the $\vec{J}_1$ unit vector by θ. Furthermore, an individual blade spins about the $\vec{I}_R$ unit vector by the angle φ. These various reference frames are depicted in Figures 3 and 4.

The unit vectors of the various reference frames are related by the following single axis transformations.

$$\begin{Bmatrix}\vec{I}_C\\ \vec{J}_C\\ \vec{K}_C\end{Bmatrix} = \begin{bmatrix}\cos(\psi_C) & \sin(\psi_C) & 0\\ -\sin(\psi_C) & \cos(\psi_C) & 0\\ 0 & 0 & 1\end{bmatrix}\begin{Bmatrix}\vec{I}_I\\ \vec{J}_I\\ \vec{K}_I\end{Bmatrix} = [T_C]\begin{Bmatrix}\vec{I}_I\\ \vec{J}_I\\ \vec{K}_I\end{Bmatrix} \tag{20}$$

$$\begin{Bmatrix}\vec{I}_1\\ \vec{J}_1\\ \vec{K}_1\end{Bmatrix} = \begin{bmatrix}\cos(\psi_T) & \sin(\psi_T) & 0\\ -\sin(\psi_T) & \cos(\psi_T) & 0\\ 0 & 0 & 1\end{bmatrix}\begin{Bmatrix}\vec{I}_I\\ \vec{J}_I\\ \vec{K}_I\end{Bmatrix} = [T_\psi]\begin{Bmatrix}\vec{I}_I\\ \vec{J}_I\\ \vec{K}_I\end{Bmatrix} \tag{21}$$

$$\begin{Bmatrix}\vec{I}_R\\ \vec{J}_R\\ \vec{K}_R\end{Bmatrix} = \begin{bmatrix}\cos(\theta) & 0 & \sin(\theta)\\ 0 & 1 & 0\\ -\sin(\theta) & 0 & \cos(\theta)\end{bmatrix}\begin{Bmatrix}\vec{I}_1\\ \vec{J}_1\\ \vec{K}_1\end{Bmatrix} = [T_\theta]\begin{Bmatrix}\vec{I}_1\\ \vec{J}_1\\ \vec{K}_1\end{Bmatrix} \tag{22}$$

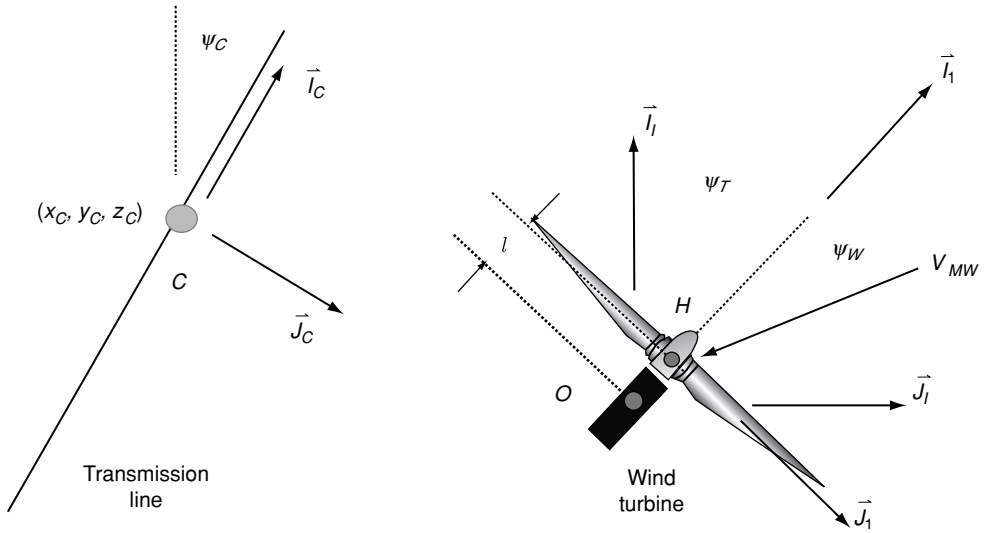

Figure 2: Wind turbine and transmission line geometry.

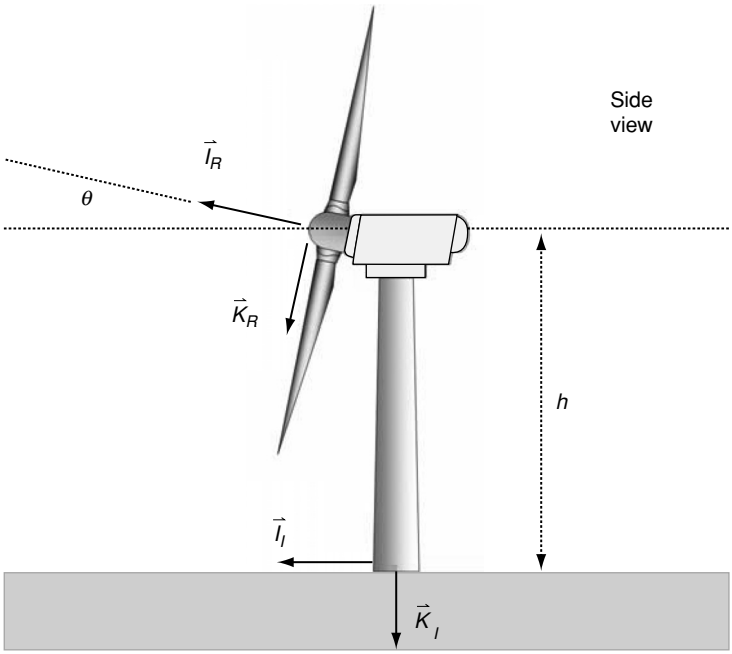

Figure 3: Side view of wind turbine.

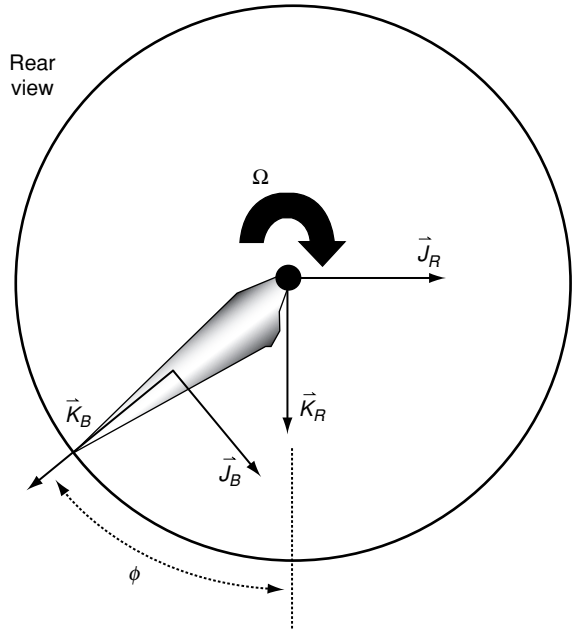

Figure 4: Rear view of wind turbine.

$$\begin{Bmatrix} \vec{I}_B \\ \vec{J}_B \\ \vec{K}_B \end{Bmatrix} = \begin{bmatrix} 1 & 0 & 0 \\ 0 & \cos(\phi) & -\sin(\phi) \\ 0 & \sin(\phi) & \cos(\phi) \end{bmatrix} \begin{Bmatrix} \vec{I}_R \\ \vec{J}_R \\ \vec{K}_R \end{Bmatrix} = [T_\phi] \begin{Bmatrix} \vec{I}_R \\ \vec{J}_R \\ \vec{K}_R \end{Bmatrix} \tag{23}$$

Thus,

$$\begin{Bmatrix} \vec{I}_B \\ \vec{J}_B \\ \vec{K}_B \end{Bmatrix} = [T_\phi T_\theta T_\psi] \begin{Bmatrix} \vec{I}_I \\ \vec{J}_I \\ \vec{K}_I \end{Bmatrix} = [T_{IB}]^T \begin{Bmatrix} \vec{I}_I \\ \vec{J}_I \\ \vec{K}_I \end{Bmatrix} \tag{24}$$

2.3. Release Conditions

At the point of release of the wind turbine rotor blade from the system, the blade is spinning about the $\vec{I}_R$ or $\vec{I}_B$ axis. Depending on the individual conditions at failure the blade can have a general orientation specified by the angles at release (φ, θ, ψ). Since the mass center of an individual blade is located off the center of rotation, it has a non-zero translational position and velocity. Moreover, since the blade is assumed to be spinning at the instant of release, it has a non-zero angular velocity as well. The state of the blade at release is used as the initial conditions for the free flight dynamic model. The position vector of the mass center at blade release is given by

$$\vec{r}_{O\to CG} = x\vec{I}_I + y\vec{J}_I + z\vec{K}_I \tag{25}$$

where

$$\begin{Bmatrix} x \\ y \\ z \end{Bmatrix} = \begin{Bmatrix} l\cos(\psi) \\ l\sin(\psi) \\ -h \end{Bmatrix} + \left[T_{IB}\right] \begin{Bmatrix} 0 \\ 0 \\ r_{CG} \end{Bmatrix} \tag{26}$$

The mass center translational velocity at release is given as

$$v_{B/I} = uI_B + vJ_B + wK_B \tag{27}$$

$$\begin{Bmatrix} u \\ v \\ w \end{Bmatrix} = \begin{Bmatrix} 0 \\ -r_{CG}\Omega \\ 0 \end{Bmatrix} \tag{28}$$

While the basic geometry of the transmission line and wind turbine system have been given in terms of rotation angles, the free flight dynamic simulation uses quaternion rotation parameters to describe orientation. The mapping from the system angles at release to initial conditions for the quaternions are given below.

$$q_0 = \cos\left(\frac{\psi}{2}\right)\cos\left(\frac{\theta}{2}\right)\cos\left(\frac{\phi}{2}\right) + \sin\left(\frac{\psi}{2}\right)\sin\left(\frac{\theta}{2}\right)\sin\left(\frac{\phi}{2}\right) \tag{29}$$

$$q_1 = \cos\left(\frac{\psi}{2}\right)\cos\left(\frac{\theta}{2}\right)\sin\left(\frac{\phi}{2}\right) - \sin\left(\frac{\psi}{2}\right)\sin\left(\frac{\theta}{2}\right)\cos\left(\frac{\phi}{2}\right) \tag{30}$$

$$q_2 = \cos\left(\frac{\psi}{2}\right)\sin\left(\frac{\theta}{2}\right)\cos\left(\frac{\phi}{2}\right) + \sin\left(\frac{\psi}{2}\right)\cos\left(\frac{\theta}{2}\right)\sin\left(\frac{\phi}{2}\right) \tag{31}$$

$$q_3 = \sin\left(\frac{\psi}{2}\right)\cos\left(\frac{\theta}{2}\right)\cos\left(\frac{\phi}{2}\right) - \cos\left(\frac{\psi}{2}\right)\sin\left(\frac{\theta}{2}\right)\sin\left(\frac{\phi}{2}\right) \tag{32}$$

Finally, the blade angular velocity at release is given by

$$\vec{\omega}_{B/I} = p\vec{I}_B + q\vec{J}_B + r\vec{K}_B \tag{33}$$

$$\begin{Bmatrix} p \\ q \\ r \end{Bmatrix} = \begin{Bmatrix} \Omega \\ 0 \\ 0 \end{Bmatrix} \tag{34}$$

To fully specify the initial condition of the rotor blade at the instant it is released from the wind turbine system requires seven parameters: l, h, r_{CG}, φ, θ, ψ, and Ω. Furthermore, the atmospheric wind velocity is defined by 2 parameters: V_{MW}, ψ_W.

2.4. Blade Impact

During simulation of a particular event, the rigid body states of the rotor blade are generated at each instant in time. This includes the position states (x, y, z), the orientation states (q_0, q_1, q_2, q_3), the translational velocity states (u, v, w), and the angular velocity states (p, q, r). These quantities can be used to compute when and where the blade impacts the ground as well as if the blade impacts a particular transmission line.

To monitor if a blade impacts a transmission line the blade root and tip position are expressed in the C reference frame (See Figure 2) relative to the origin of the C reference frame as

$$\vec{r}_{C\to ROOT} = \vec{r}_{C\to O} + \vec{r}_{O\to ROOT} = x_{ROOT}\vec{I}_C + y_{ROOT}\vec{J}_C + z_{ROOT}\vec{K}_C \tag{35}$$

where,

$$\begin{Bmatrix} x_{ROOT} \\ y_{ROOT} \\ z_{ROOT} \end{Bmatrix} = [T_C]\left[\begin{Bmatrix} x-x_C \\ y-y_C \\ z-z_C \end{Bmatrix} + [T_{IB}]\begin{Bmatrix} 0 \\ 0 \\ r_{ROOT}-r_{CG} \end{Bmatrix}\right] \tag{36}$$

$$\vec{r}_{C\to TIP} = \vec{r}_{C\to O} + \vec{r}_{O\to TIP} = x_{TIP}\vec{I}_C + y_{TIP}\vec{J}_C + z_{TIP}\vec{K}_C \tag{37}$$

$$\begin{Bmatrix} x_{TIP} \\ y_{TIP} \\ z_{TIP} \end{Bmatrix} = [T_C]\left[\begin{Bmatrix} x-x_C \\ y-y_C \\ z-z_C \end{Bmatrix} + [T_{IB}]\begin{Bmatrix} 0 \\ 0 \\ r_{TIP}-r_{CG} \end{Bmatrix}\right] \tag{38}$$

with r_{CG} being the distance from the hub H to the blade mass center, r_{ROOT} being the distance from the hub H to the blade root, and r_{TIP} being the distance from the hub H to the blade tip. Viewing the blade along the transmission line yields a two dimensional problem. In Figure 5, the angle γ_{RT} can be computed using

$$\gamma_{RT} = \tan^{-1}\left(\frac{z_{TIP}-z_{ROOT}}{y_{TIP}-y_{ROOT}}\right) \tag{39}$$

To compute the minimum distance of the transmission line to a point on the blade, the point C is expressed in the RT reference frame. Let the component of this position vector along $\vec{J}_{RT}$ be denoted at $\tilde{y}$ and the component along $\vec{K}_{RT}$ be denoted as $\tilde{z}$. If $0 < \tilde{y} < r_{TIP} - r_{ROOT}$ then the minimum separation distance between the blade and the transmission line is $|\tilde{z}|$. Otherwise, the minimum separation distance is either the distance from the transmission line to the blade root or the distance from the transmission line to the blade tip. When the minimum distance from the transmission line and the rotor blade is within a prescribed tolerance of half the blade chord, the rotor blade is said to impact the transmission line.

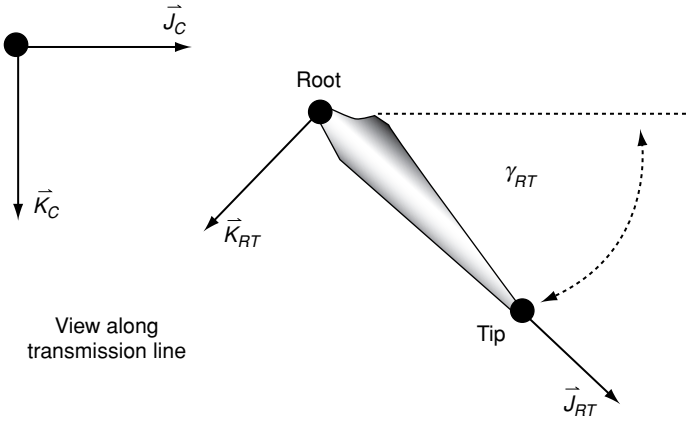

Figure 5: View of rotor blade along the transmission line.

3. RESULTS

3.1. System Description

In order to exercise the above risk modeling methodology, a generic 1.5 MW wind turbine system is considered. Basic data for the wind turbine system is presented in Table 1.

Aerodynamic lift and drag coefficient data was obtained by blending low angle of attack data for the S825 and S826 wind turbine airfoils reported by Somers [10] with generic high angle of attack data for the NACA 0012 airfoil [11]. Since the blade is in free flight when released and the blade can attain angles of attack from 180 deg to –180 deg, it is important to have a wide range of angle of attack capability in the dynamic model. Generalized blade twist and chord distributions are based on the work of Griffin [12].

For the reported results, five different blade fragment sizes were considered, including a full blade throw (100% blade), outer 80% blade throw, outer 60% blade throw, outer 40% blade throw, and outer 20% blade throw. Also for each simulation a total of 144 transmission lines were evaluated (36 different distances from the hub in each of the four directions). Schematics of the transmission lines considered are provided in Figures 6, 7, and 8. Figure 6 shows North, South, East, and West transmission lines. The North and South transmission lines are positioned upwind (North) and downwind (South) of the wind turbine. The East and West transmission lines are adjacent to the wind turbine. The transmission line offset from the wind turbine is measured from the center of the wind turbine tower to the transmission line (d). Since the wind turbine blades rotate in the $\vec{J}_I - \vec{K}_I$ plane just before failure and subsequent

Table I: Basic wind turbine data

Parameter	1.5 MW Turbine
Blade Radius (m)	35
Blade Weight (N)	49,050
r_{CG} (m)	17.5
Blade I_{xx} ($kg–m^2$)	511,000
Blade I_{yy} ($kg–m^2$)	510,000
Blade I_{zz} ($kg–m^2$)	1,233
Ω (rad/s)	–2.3
Tower Height h (m)	80.0
Tower Offset l (m)	1.72
Root Blade Chord (m)	2.1
Tip Blade Chord (m)	0.94
Root Blade Pitch (deg)	10.5
Tip Blade Pitch (deg)	–0.5
Air Density ρ (kg/m^3)	1.2

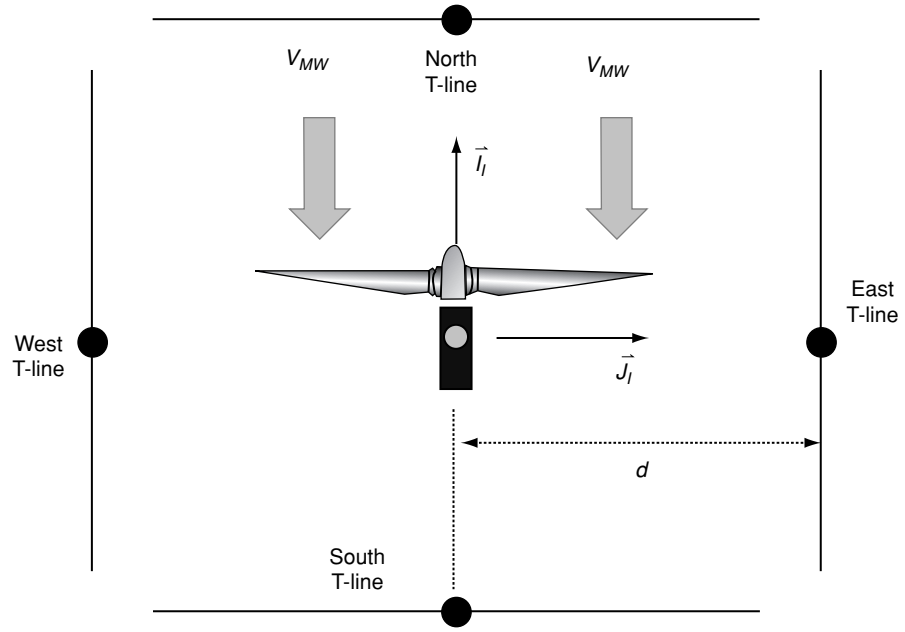

Figure 6: Overhead schematic of transmission line and wind turbine system.

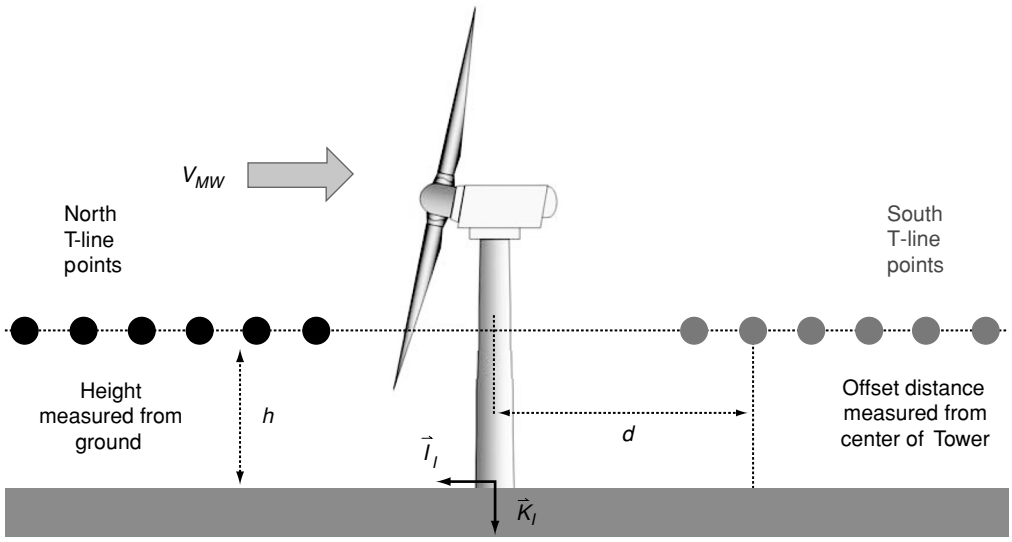

Figure 7: Side view of transmission line and wind turbine system.

release, the blades tend to be thrown along the $\vec{J}_I$ axis. Figure 7 shows a side view of the overall transmission line and wind turbine system with several North and South transmission lines depicted. Likewise, Figure 8 presents a front view with several East and West transmission lines depicted.

3.2. Example Single Trajectory

Figures 9 through 13 present a typical single trajectory for a 100% blade fragment throw from a generic 1.5 MW wind turbine blade. Figures 9 and 10 show a rear and side view of the mass center trajectory with a single east transmission line at a distance d of 95 m and a height h of 40 m. The overall trajectory duration is just over 3.1 sec from blade release to ground impact. The blade is released at an azimuth position of $-\pi/4$ rad while rotating at –2.3 rad/s. The blade

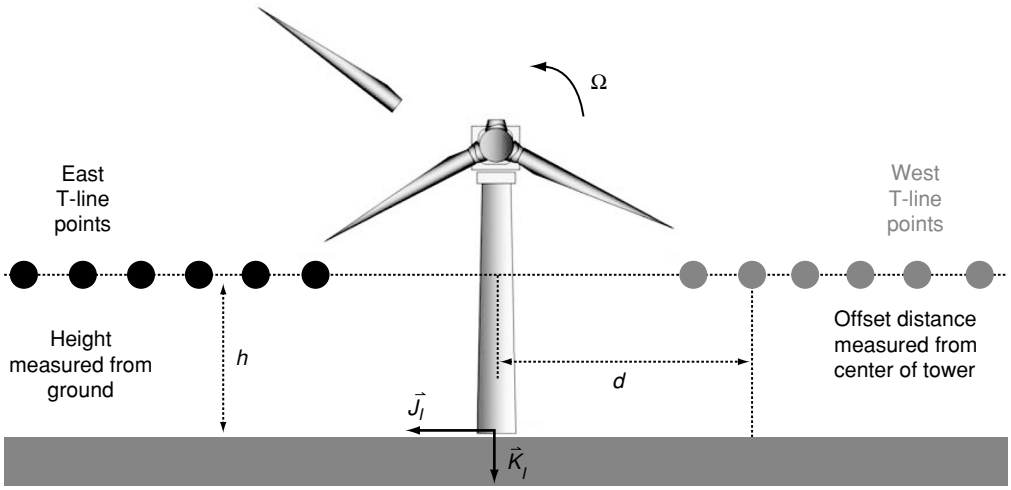

Figure 8: Front View of transmission line and wind turbine system.

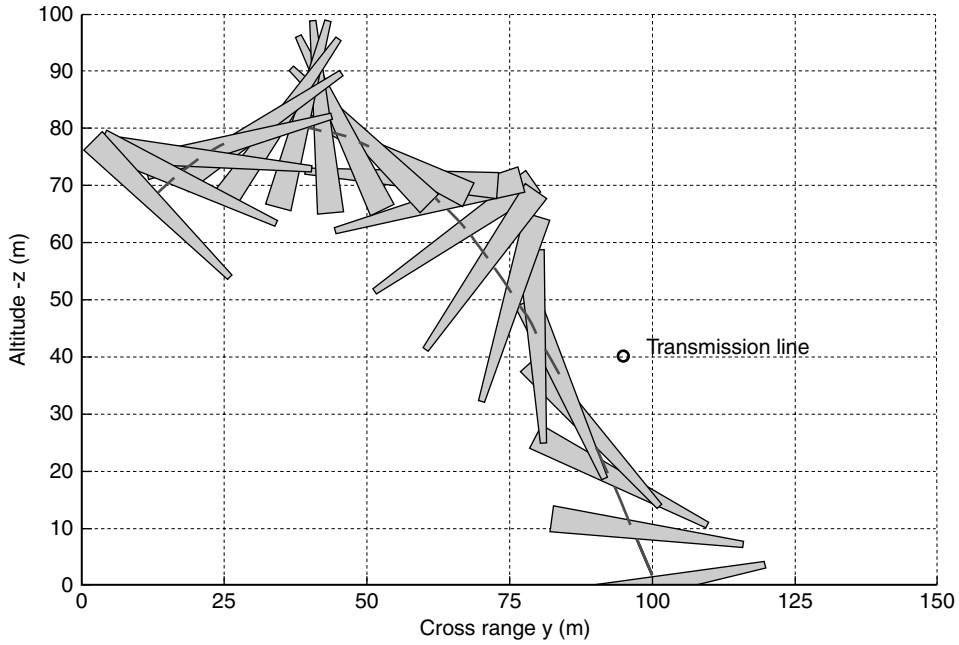

Figure 9: Example trajectory rear view (1.5 MW Wind Turbine, 100% Blade Throw).

trajectory mainly occurs in the cross range direction where there is 101 m of total travel whereas the range direction shows approximately 28 m of travel. Figure 9 demonstrates the importance of including the rotor blade orientation when considering setback standards. In the example trajectory the rotor blade clearly misses impacting the transmission line as the mass center passes within 15 m of the line. However, the failure to impact the transmission line is not because of the rotor blades lack of proximity to the line but rather rotation as it passes. It can be seen that if the rotation is advanced or retarded by $\pi/2$ rad impact is likely.

The quaternion orientation parameters are shown in Figure 11 where a gentle rotation about $\vec{I}_I$ is exhibited. The body angular velocities are plotted in Figure 12 where relatively constant angular rates are shown. Figure 13 plots the total inertial velocity of the mass center of the blade. The total velocity decreases from 40 m/s to 30 m/s as the blade initially increases in altitude before increasing to 75 m/s as it impacts the ground.

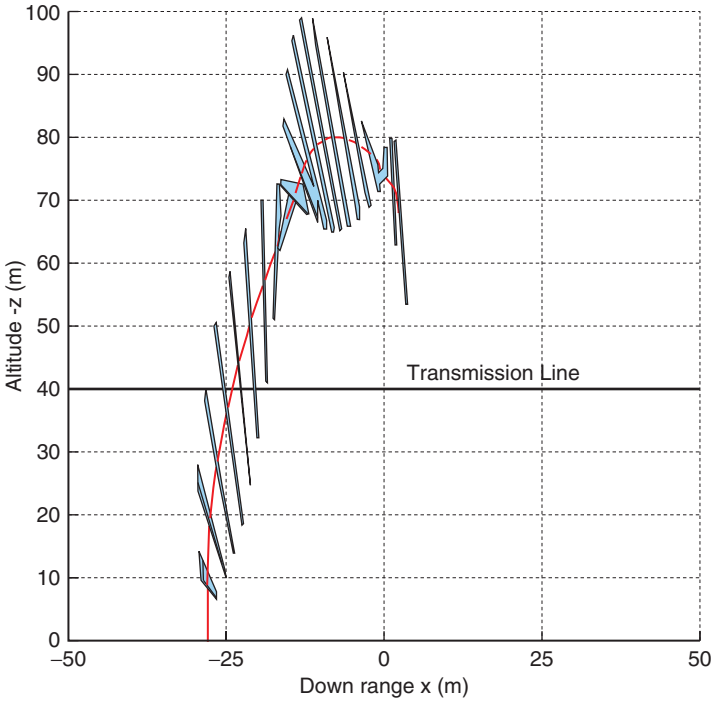

Figure 10: Example trajectory side view (1.5 MW Wind Turbine, 100% Blade Throw).

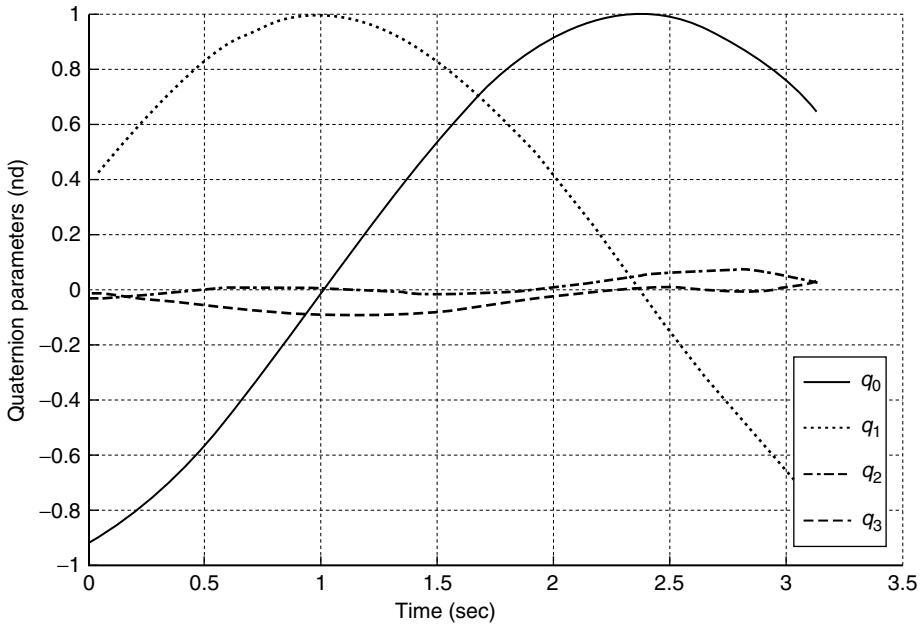

Figure 11: Example trajectory orientation parameters (1.5 MW Wind Turbine, 100% Blade Throw).

3.3. Example Monte Carlo Simulation

The trajectory of a failed wind turbine rotor blade is a complex function of many parameters, including but not limited to atmospheric wind velocity and direction, rotor radius, tower height, rotor rotational speed, rotor blade mass and inertia, and rotor incidence and flapping angles. Release of failed wind turbine rotor blade can occur at an arbitrary point in time during operation. At different points in a revolution the blade attains different states, yielding different release conditions. For the Monte Carlo simulation data presented below,

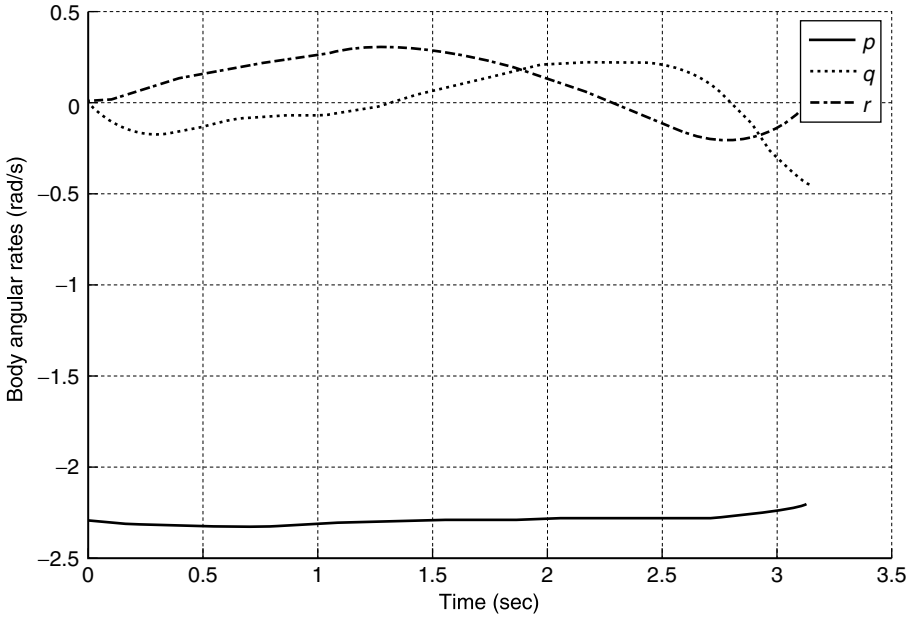

Figure 12: Example trajectory angular rates (1.5 MW Wind Turbine, 100% Blade Throw).

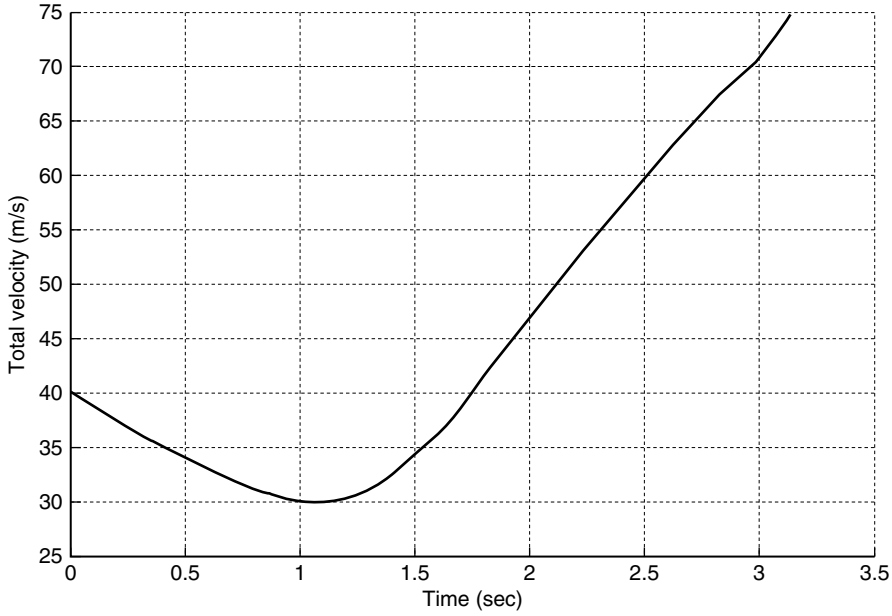

Figure 13: Example trajectory total velocity (1.5 MW Wind Turbine, 100% Blade Throw).

6 parameters are randomized, namely, φ, θ, ψ, Ω, V_W, and ψ_W. Each of these parameters possesses a statistical distribution for typical wind energy system installations (Table II). A sample size of 10000 was used for all cases reported.

These different release conditions lead to different individual trajectories and associated ground impact points. In Monte Carlo simulation, all key parameters that can vary at release are considered random variables with known statistical properties. For each random variable, a set of samples is created such that the samples exhibit the proper statistical

Table II: Monte Carlo simulation random parameter statistics

Parameter	Mean	Standard Deviation
φ - Roll Angle (deg)	0	-180 to 180(uniform)
θ - Cant Angle (*deg*)	4	1.0
ψ - Azimuthal Angle	0	10.0
Ω - Rotational Speed	–2.3	0.1
V_W - Wind Velocity	14	3.0
ψ_W - Wind Angle (*deg*)	0	3.0

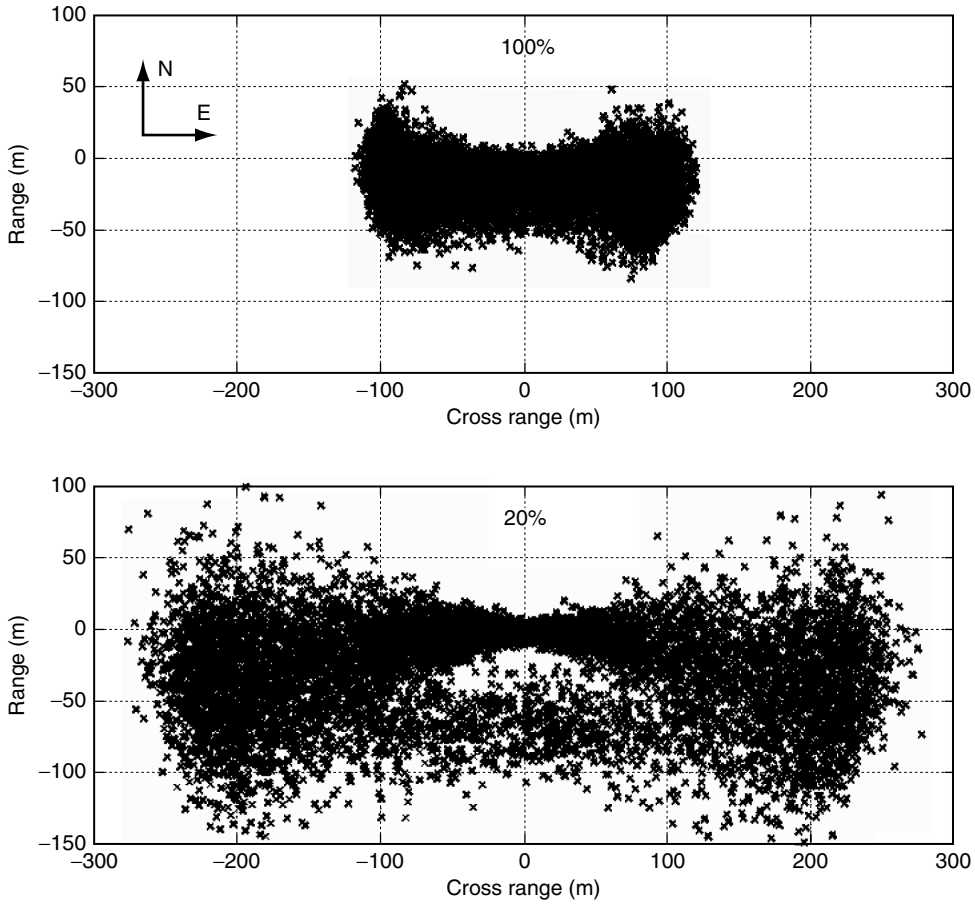

Figure 14: Monte Carlo simulation ground impact points (1.5 MW Wind Turbine 100% and 20% blade failure).

distribution. For each entry in the sample, a rotor blade free flight trajectory is computed and for each trajectory the minimum distance of the blade with respect to a transmission line is obtained along with the associated ground impact point.

Figures 14 through 17 present results for a typical Monte Carlo simulation. In each figure results for a 100% and 20% blade throw from a 1.5 MW wind turbine blade are shown. The 100% blade throw case represents a situation where the blade fails at the root and the entire rotor blade is thrown into atmosphere flight. The 20% blade throw case represents a situation where the outer 20% of the rotor blade is released into atmospheric flight. Figure 14 shows a top view of ground impact points. Notice that for 100% the scatter along the cross range direction is bounded by +/– 110 m while scatter along the range direction is –70 m to 50 m. The scatter for

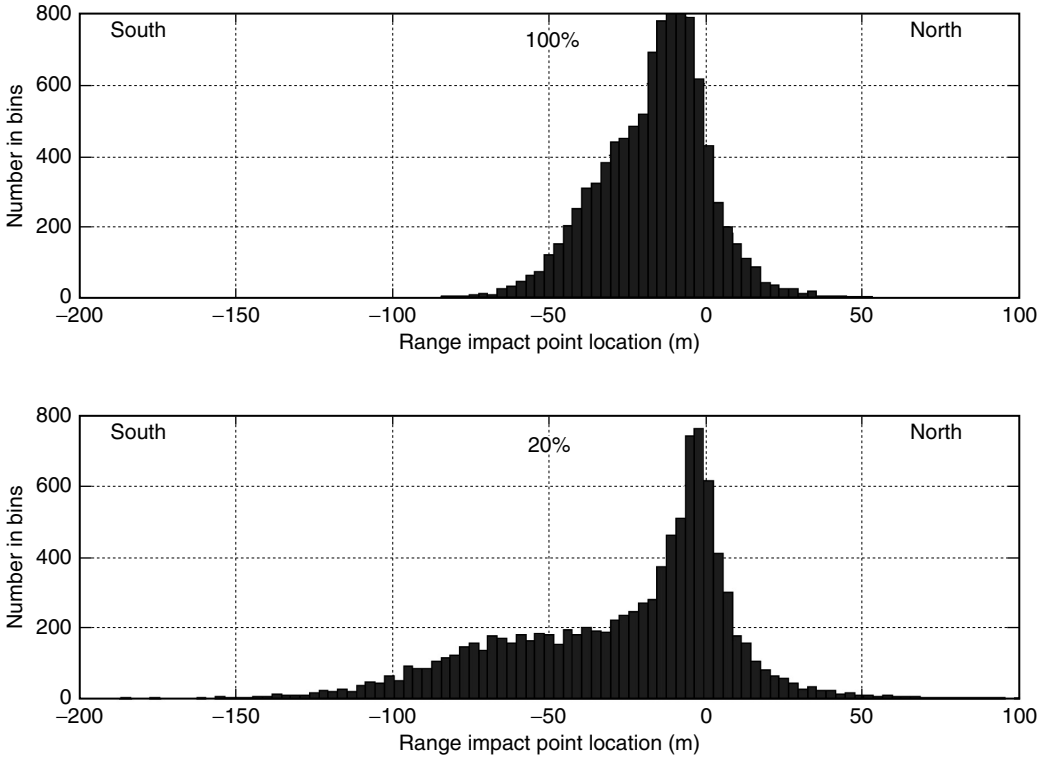

Figure 15: North-south impact histogram (1.5 MW Wind Turbine 100% and 20% blade failure).

the smaller 20% failures along the cross range direction is bounded by +/– 280 m while scatter along the range direction is –150 m to 100 m. Figures 15 and 16 present histograms of the range and cross range mass center impact point. The range histogram (Figure 15) shows a single peak occurring slightly down wind of the wind turbine. On the other hand, the cross range histogram (Figure 16) exhibits a peak on both the east and west sides as well as a peak slightly down. Figure 17 plots the probability of a transmission line impact given a wind turbine blade throw as a function of the distance of the transmission line from the center of the wind turbine tower. For 100% blade failure impacts on the North and South transmission lines, the probability of impact steadily decreases as the offset distance from the wind turbine tower and transmission line grows. On the other hand, the East and West transmission lines exhibit a peak in the probability of impact at a certain offset distance. The probability of transmission line impact for 100% blade failure reaches zero for offset distance greater than 100 m for all cases. In contrast for the 20% blade failure, while the probability is generally much smaller, the probability of transmission line impact remains nonzero past 100 m offset distance due to the larger impact footprint shown in Figure 14.

3.4. Parametric Trade Study Results

As discussed above, Monte Carlo simulations were performed for a representative 1.5 MW turbine and 5 different blade fragment percentages (100%, 80%, 60%, 40%, 20%). Figure 18 presents the probability of impact for the North, East, South, and West transmission lines as a function of the transmission line offset distance and blade fragment size. All results are shown for a transmission line height of 50 m. Since the North transmission line is upwind of the wind turbine, very few blades are thrown toward this transmission line resulting in an exceedingly

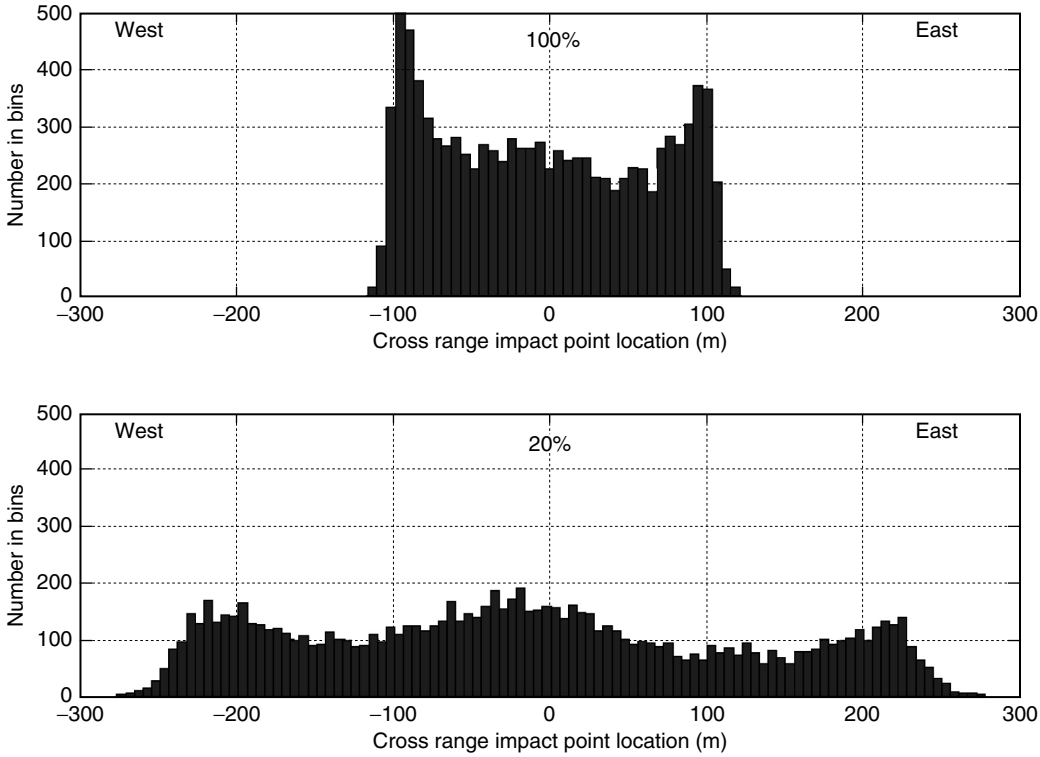

Figure 16: East-west impact histogram (1.5 MW Wind Turbine 100% and 20% blade failure).

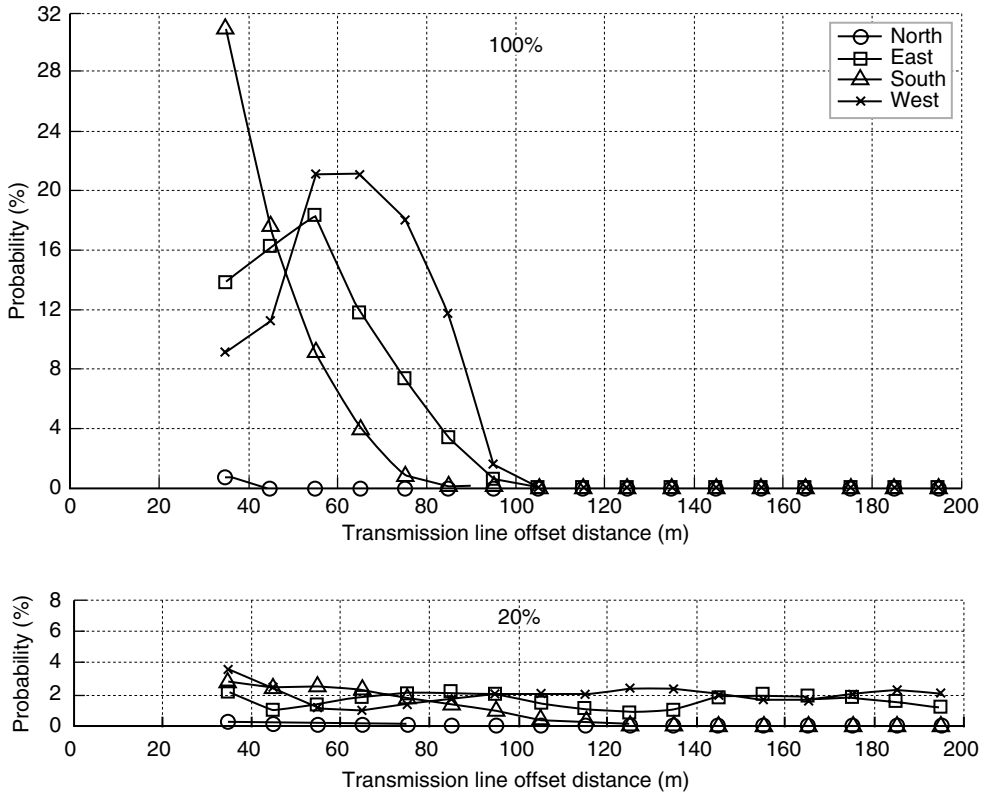

Figure 17: Transmission line impact probability (1.5 MW Wind Turbine 100% and 20% blade failure).

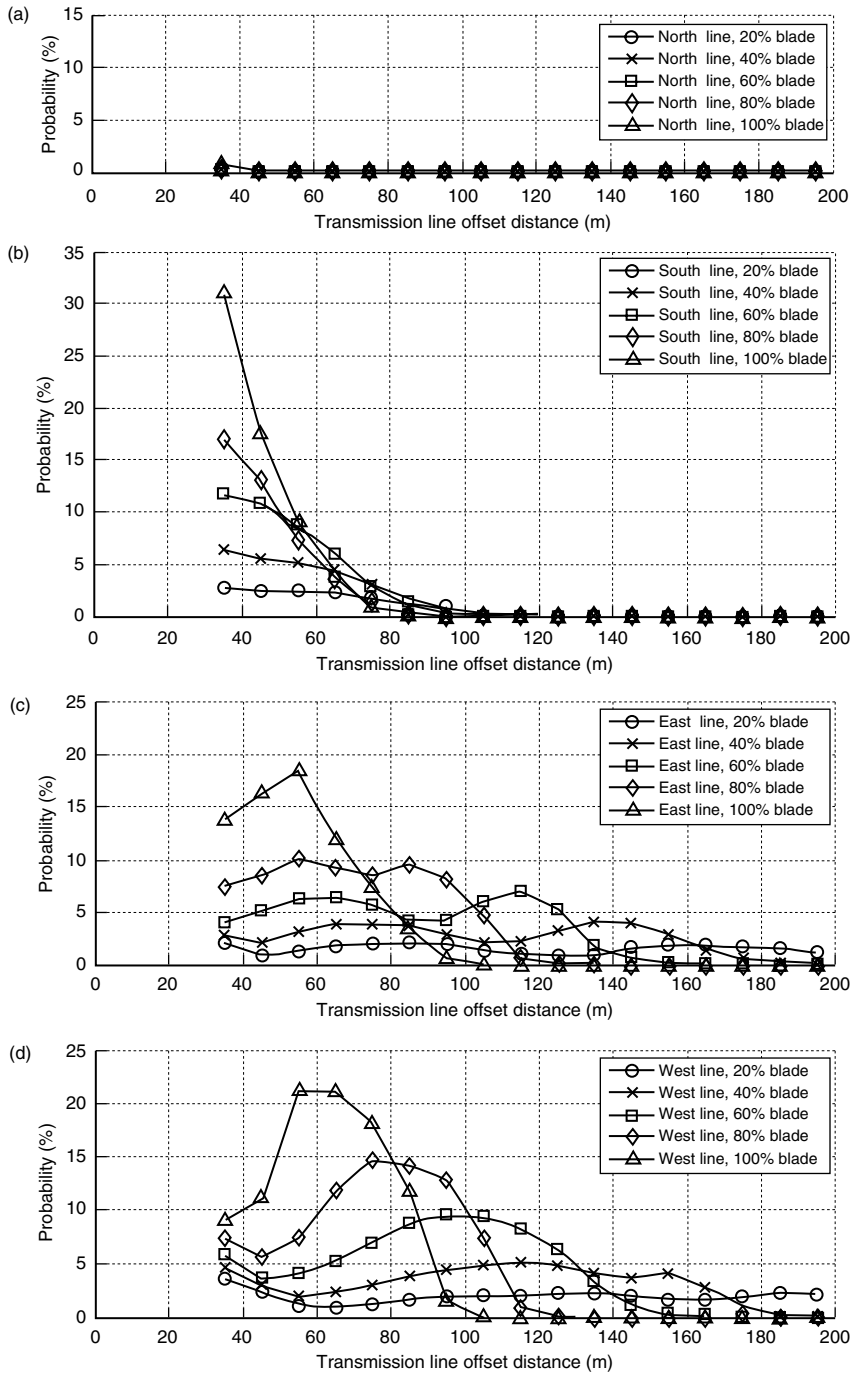

Figure 18: 1.5 MW wind turbine transmission line impact probabilities. (a) North, (b) South, (c) East, (d) West.

small probability of transmission line impact (Figure 18 a). On the other hand, the East transmission line is adjacent to the wind turbine and results in many more transmission line impact events (Figure 18 c). It is interesting to note that the larger blade fragments have higher maximum probability of line impact over a small transmission line offset range while small blade fragments have lower maximum probability spread out over a large band of transmission line offset distances. Also, the envelope of maximum probability of line impact

decreases in an exponential fashion as a function of transmission line offset distance. Since the South transmission line is downwind of the wind turbine, failed blades get blown downstream and can impact the South transmission line (Figure 18 b). Notice that the probability of impact steadily decreases as a function of transmission line offset distance for all blade fragment sizes. The West transmission line results largely follow the trends contained in the East transmission line results (Figure 18 d).

4. CONCLUSIONS

The probability that a failed wind turbine blade which is released into the atmosphere will impact a power transmission line is examined in detail in this report through computer simulation. A comprehensive flight dynamic simulation tool comprised of a rigid body representation with 6 degrees of freedom is employed. The model generates full three dimensional motion of a failed wind turbine blade from release of the wind turbine blade at the point of failure to impact. Motion of the failed wind turbine blades are driven by the initial conditions at failure, gravity, and aerodynamic forces and moments. Monte Carlo simulation is used to generate impact statistics. A comprehensive set of simulation results are generated for a nominal 1.5 MW wind turbine and 50 m transmission line height. Results are obtained as a function of the transmission line offset distance from the wind turbine tower and as a function of the size of the blade fragment that is thrown. The reported methodology provides a means to assess the risk that a failed wind turbine blade or blade fragment will impact a power transmission line for a specific wind turbine and transmission line geometry.

Results from the simulation study confirm some intuitive notions regarding blade impact on a transmission line. The impact probability decreases as the wind turbine tower and transmission line offset distance increases. The transmission line location and orientation have a large impact on resulting impact probability characteristics. Transmission lines perpendicular to the blade rotation plane (East/West) yield higher impact probability than parallel transmission line location and orientations (North/South). Small and light blade fragments fly further than large and heavy blade fragments. Interestingly, large blade fragments fly short, but due to their size tend to impact transmission lines more frequently than a similar small fragment at the same transmission line offset distance. Large fragments have higher transmission line impact probability at relatively small transmission line offset distance while small fragments have higher probability of line impact at larger transmission line offset distance. The envelope on impact probability for all blade fragment sizes exhibits an exponentially decaying behavior as a function of transmission line offset distance.

REFERENCES

1. Tavner PJ, Xiang J, Spinato F. Reliability Analysis for Wind Turbines. *Wind Energy* 2007; **10**:1–18. DOI: 10.1002/we.204.
2. Eggwertz S, Carlsson I, et al. Safety of Wind Energy Conversion Systems with Horizontal Axis. Stockholm, *Flygtekniska Försöksanstalten (FFA -The Aeronautical Research Institute of Sweden)*. Technical Note HU-2229 1981.
3. Macqueen J, Ainsilie J, et al. Risks associated with wind turbine blade failures. *IEE Proceedings 130* 1983; Part A(9) 574–586.
4. Turner D. A Monte Carlo Method for Determining the Risk Presented by Wind Turbine Blade Failures. *Wind Engineering* 1986; **11**(1): 1–20.

5. Eggers A, Holley W, et al. Exploratory Study of HAWT Blade Throw Risk to Nearby People and Property. *ASME Wind Energy Symposium* Reno, Nevada, pp 355–367, 2001.

6. Montgomerie B. Horizontal Axis Wind Turbine Blade Failure, Blade Fragment Six Degrees of Freedom Trajectory, Site Risk Level Prediction. *Fourth International Symposium on Wind Energy Systems*, Stockholm, Sweden, HRA Fluid Engineering, pp 389–401, 1982.

7. Sørensen J. On the Calculation of Trajectories for Blades Detached from Horizontal Axis Wind Turbines. *Wind Engineering* 1984; **8**(3): 160–175.

8. Sørensen J. Prediction of Site Risk Levels Associated with Failures of Wind Turbine Blades. *European Wind Energy Conference*, Hamburg, Germany, H.S. Stephens & Associates, pp. 344–349, 1984.

9. Turner D. An Analysis of blade throw from wind turbines. *Wind Energy and the Environment*. P.D.T. Swift-Hook, London, Peter Peregrinus, Ltd, 1989; 112–135.

10. Somers D. The S825 and S826 Airfoils. *National Renewable Energy Laboratory, Subcontractor Report* NREL/SR-500-36344, Subcontract Number DE-AC36-99-GO10337, 2005.

11. Prouty R. Helicopter Performance, Stability, and Control. *Wadsworth Publishing Company*. 1986, ISBN 0534063608 / 0-534-06360-8

12. Griffin D. Blade System Design Studies Volume II: Preliminary Blade Designs and Recommended Test Matrix. *Sandia Report Number SAND2004-0073*, Sandia National Laboratories, Albuquerque, NM, 2004.